

Torque ripple reduction design of Multi-layer Interior Permanent Magnet Synchronous Motor by using Response Surface Methodology

Liang Fang, Soon-O Kwon, Peng Zhang, Jung-Pyo Hong, *Senior Member IEEE*

Abstract—In this paper, multi-layer interior permanent magnet design is proposed for the torque ripple reduction design in an conventional single layer interior permanent magnet synchronous motor(IPMSM). With the help of optimization analysis in response surface methodology(RSM), the reduction of the torque ripple in the IPMSM multi-layer design is achieved by improving the characteristics of the Total harmonic distortion(THD)of the back e.m.f and the cogging torque. The validity of multi-layer IPM design for reducing the torque ripple of the IPMSM is well proved by finite element analysis results comparison between the prototype single layer IPMSM and the multi-layer designed IPMSM model.

Index Terms—multi-layer design, Torque ripple reduction, RSM, THD of Back e.m.f, Cogging torque, FEA.

I. INTRODUCTION

IN recent years, interior permanent magnet synchronous machines(IPMSM) have been widely used in public welfare and the industrial field for their many advantages, such as high torque density, high efficiency and high quantity output[1].

On the other hand, the IPM machines have significant torque ripple production, which causes serious operating noise and vibration. For getting a satisfied output torque performance, the torque ripple should be reduced. There are many kinds of design approach presented in the literature for reducing the torque ripple. In this paper, multi-layer IPM design is introduced as the approach of torque ripple reduction design[2],[3].

Single layer IPM synchronous machines as the simplest IPM design, were the first to be implemented and put into production[4]. With the development of IPMSM, multi-layer

Manuscript received April 24, 2006. This work was supported by grant No. RTIO4-O1-O3 from the Regional Technology Innovation Program of the Ministry of Commerce, Industry and Energy (MOCIE)

Liang, Fang is with the Department of Electrical Engineering, Changwon National University, #9 Sarim-dong, Changwon, Gyeongnam, 641-773, KOREA (phone: 82-055-2625966; fax: 82-055-2625965; e-mail: fangliangcw@hotmail.com)

Soon-O Kwon, Peng, Zhang are with the Department of Electrical Engineering, Changwon National University, KOREA (phone: 82-055-2625966; fax: 82-055-2625965; e-mail: kso1975@changwon.ac.kr, zp002597@hotmail.com)

Jung-Pyo Hong is with the Department of Electrical Engineering, Changwon National University, KOREA (phone: 82-055-2625966; fax: 82-055-2625965; e-mail: jphong@changwon.ac.kr).

IPM design attracts more and more interests. Compare with the single layer designs, multi-layer IPM designs can effectively improve the machines performance further.

Firstly, a single layer IPMSM applied for household air-condition used is introduced as the prototype model. The quite important characteristic of this IPMSM is that it should run quietly, low noise and vibration. Correspondingly, the performance of the output torque must have low torque ripple.

As we know, the torque ripple is caused by the construction of the magnetic circuit of a machine mainly from[5]:

- Distortion of the sinusoidal distribution of the magnetic flux in the air gap;
- CT effect, i.e., interaction between the rotor magnetic flux and variable permeance of the geometry of stator slots;
- Difference of permeances between the d-axis and q-axis.

In this paper the torque ripple reduction with the multi-layer IPM design is achieved through the Total harmonic distortion(THD) of the back e.m.f (called back_e.m.f THD for common) and cogging torque(CT) improvement. Both of them have obvious effect on the toque ripple pulsation. At the same time, the quantity of the output performance can be ensured.

With the help of Design of Experiment(DOE) and Response Surface Methodology(RSM) analysis, the optimization of the characteristics both the back e.m.f THD and CT can be easily investigated. The finite element method(FEM) is used for analyzing the characteristics of the IPMSM in this paper.

II. MODEL ANALYSIS AND DESIGN

A. Prototype IPMSM Model

The existing prototype IPMSM model is presented in Fig. 1. It has 4-pole and 6-slot, with a single PM layer buried inside the rotor part for each pole.

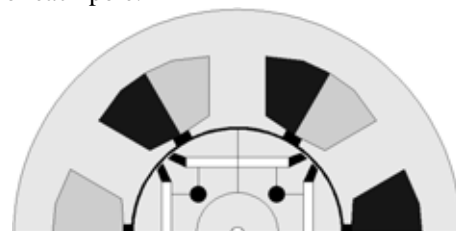


Fig. 1 Prototype single layer IPMSM model

B. Prototype IPMSM Characteristic Analysis

Firstly, the concerned characteristics for optimization analysis of the prototype IPMSM model are analyzed by the FEM calculation. The torque ripple of the prototype IPMSM model achieves 25.34%, with the characteristics of back e.m.f THD (9.44%) and CT (peak-to-peak value is 1.374 Nm), which can be found in the Fig. 10 and Fig. 11. This prototype IPMSM has serious noise and vibration. In order to overcome this problem, the torque ripple should be reduced without destroying the output performance. Therefore, the motor characteristics of back e.m.f THD and CT are chosen for torque ripple reduction design.

III. DOUBLE LAYER IPMSM DESIGN

A. Design of Experiment (DOE)

In the multi-layer IPM design, more design variables are created in the nature of things. In this multi-layer IPM design, double layer IPM construction is chosen for the torque ripple reduction because of the considerations such as the simplicity for manufacturing, the easiness of inserting PM into the rotor core and the mechanical robustness.

The design variables of double layer IPMSM model are defined as the following Fig. 2 (a) and (b) show. There exits two PM layers each pole in the core, and a pair of flux barriers each PM layer. Therefore, the angles of each flux barrier pairs (α, β) are selected. And, the relative division of these 2 layers of buried PM is considered by taking the variable (γ), which is defined as the angle of the each layer tip connected line, when the gap between the two layers is fixed at 5(mm) for rotor strength consideration. In the DOE design, all of these three design variables (α, β, γ) are investigated in term of angle among the range of $[30^\circ \sim 60^\circ]$.

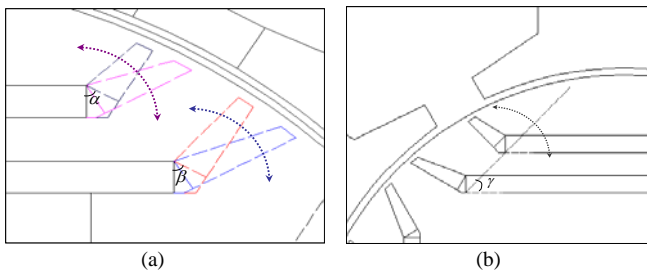


Fig. 2 double layer IPM design variables in the rotor part: (a) flux barrier angle (α, β); (b) PM layer tip line angle (γ).

Table.1 DOE Full factorial Design Array

No.	α	β	γ	CT	THD
1	45	45	45	0.29400	0.10208
2	30	30	60	0.30194	0.03753
3	60	30	60	0.59309	0.06145
4	60	30	30	0.30844	0.21805
5	60	60	30	0.60607	0.11528
6	30	60	60	0.23140	0.07328
7	60	60	60	0.29450	0.08736
8	30	30	30	0.44155	0.18451
9	30	60	30	0.64790	0.09777

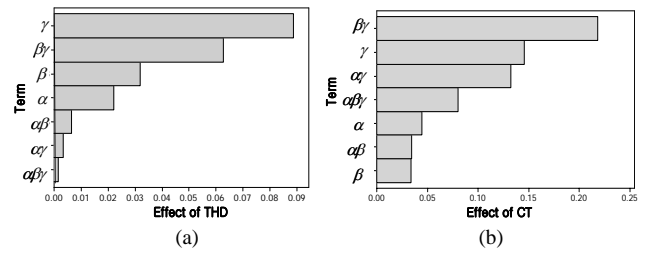


Fig. 3 Standardized Effects : (a) Back e.m.f THD and (b) Cogging torque (CT)

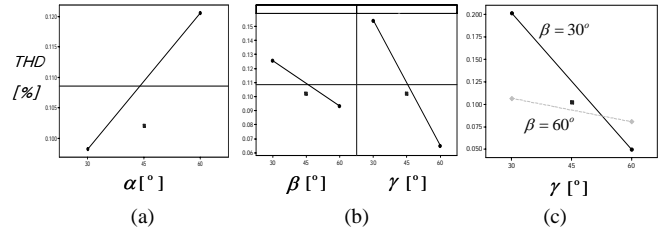


Fig. 4 Back e.m.f THD Effects analysis : (a) α main effect; (b) $[\beta, \gamma]$ main effect; (c) $[\beta, \gamma]$ interaction effect

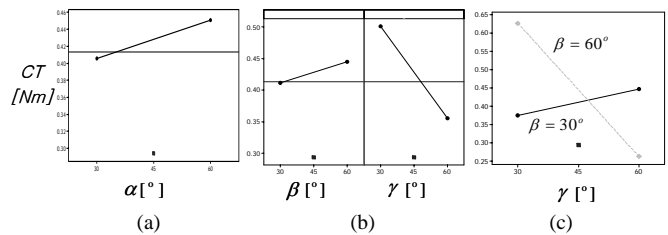


Fig. 5 Cogging torque Effect analysis : (a) α main effect; (b) $[\beta, \gamma]$ main effect; (c) $[\beta, \gamma]$ interaction effect

From the Fig. 3 Effect Pareto charts analysis, the design variables (β, γ) have greater effect on both back e.m.f THD and CT characteristics, therefore (β, γ) are selected for further investigation later. On the other hand, the design variable α is excluded from the main design variable analysis.

In the DOE analysis, the design variables are investigated from both main effect and interaction effects[6], as the Fig. 4 and Fig. 5 display. According to the variation of back e.m.f THD and CT plots, the fittest values can be found primarily.

From the experimental research, compare with the CT effect on the torque ripple, back e.m.f THD has a relative larger ripple pulsation, therefore the THD characteristic should be firstly considered in the design variable effects analysis. The main design variables (β, γ) are analyzed from the (b) and (c) of the Fig. 4. When ($\beta=30^\circ, \gamma=60^\circ$), the minimum of back e.m.f THD can be obtained. Also, from Fig. 5 (b), design variable γ shows great effect on the reduction of CT. When the ($\gamma=60^\circ$), the CT can be obviously reduced. At the same time, the design variable (α) should be fixed at ($\alpha=30^\circ$) for getting the minimum values of both back e.m.f THD and CT from the Fig. 4(a) and Fig. 5(a) analysis. Therefore, in the DOE part, the main design variables (β, γ) and the anticipatory optimization design area ($\alpha=30^\circ, \beta=30^\circ, \gamma=60^\circ$) can be concluded.

B. Response Surface Methodology (RSM)

RSM is a collection of statistical and mathematical techniques used for developing, improving and optimizing process[6]. According to the DOE analysis, the selected main

design variables (β, γ) are investigated near the pre-determined point ($\alpha=30^\circ, \beta=30^\circ, \gamma=60^\circ$). The experimental array of the RSM is listed in Table. 2, and the characteristics of THD and CT with each combination of design variables are calculated by FEM.

Table. 2 Experimental Array of RSM

No.	γ	β	CT	THD
1	60.0000	30.0000	0.51094	0.05132
2	45.8579	30.0000	0.52431	0.06875
3	60.0000	30.0000	0.51094	0.05132
4	50.0000	40.0000	0.44898	0.08510
5	60.0000	15.8579	0.52431	0.06875
6	70.0000	20.0000	0.24660	0.05113
7	60.0000	44.1421	0.38151	0.05700
8	60.0000	30.0000	0.51094	0.05132
9	74.1421	30.0000	0.17647	0.04929
10	60.0000	30.0000	0.51094	0.05132
11	50.0000	20.0000	0.52327	0.10488
12	70.0000	40.0000	0.20090	0.05404
13	60.0000	30.0000	0.51094	0.05132

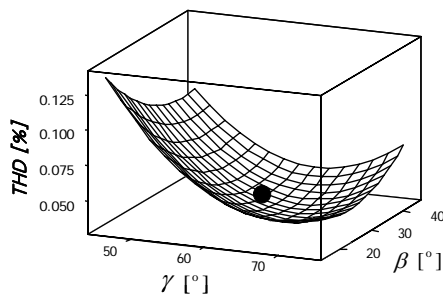


Fig. 6 response surface of Back e.m.f value

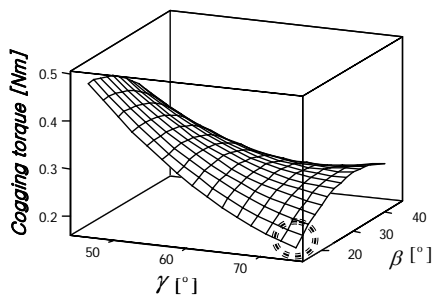


Fig. 7 response surface of Cogging torque (CT) value

New D	Hi	γ	β
0.97533	Cur	74.1421	44.1421
	Lo	[68.0]	[31.40]
		45.8579	15.8579
CT			
Minimum			
y = 0.2677			
d = 1.0000			
THD			
Minimum			
y = 0.0333			
d = 0.95128			

Fig. 8 Optimal design variables and responses analysis

Then, the variation of the characteristics back_e.m.f THD and CT can be observed from the response surfaces as the Fig. 6 and Fig. 7 show. In the response surfaces, the optimal region can be directly determined. But the optimal result each response is not achieved with the same design variables. Therefore, the interaction responses are analyzed in the Fig. 10 and the optimal design variables are obtained properly.

IV. RESULT COMPARISON

In the RSM analysis, the improved characteristics of the optimal designed double layer IPMSM are obtained theoretically, which gave the results that back_e.m.f THD (3.33%) and CT ($Peak.=0.2677(Nm)$), when ($\alpha=30^\circ, \beta=31.4^\circ, \gamma=68.0^\circ$). But on the other hand, RSM is a kind of analytical method in essence, with inevitable error existing in the obtained results[7]. Therefore, it is necessary that the double layer designed IPMSM model is established with the design variables combination [$\alpha=30^\circ, \beta=31.4^\circ, \gamma=68^\circ$], and the characteristics of the new designed model are precisely calculated by FEM.

The redesigned double layer IPMSM model is built in Fig. 9, with the determined design variables from RSM. And then, the characteristics of this new designed IPMSM model are calculated by the FEM. In the Fig. 10 and Fig. 11, the back e.m.f THD and CT plots of the double layer IPMSM are compared with the prototype model. It can be found, that the THD value is decreased from 9.44% to 3.47%, and the CT values are decreased from 1.374(Nm) to 0.367(Nm). Finally, the torque ripple of the output is compared in Fig. 12. After the optimal design, the torque ripple is decreased from 25.34% to 17.55%, nearly 30% improvement, and with a certain increase of average output torque.

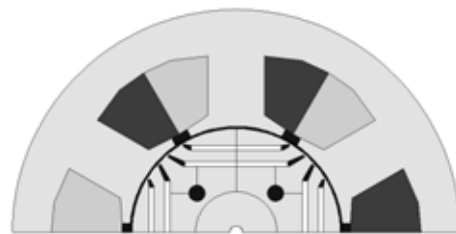


Fig. 9 Optimal redesigned double layer IPMSM model

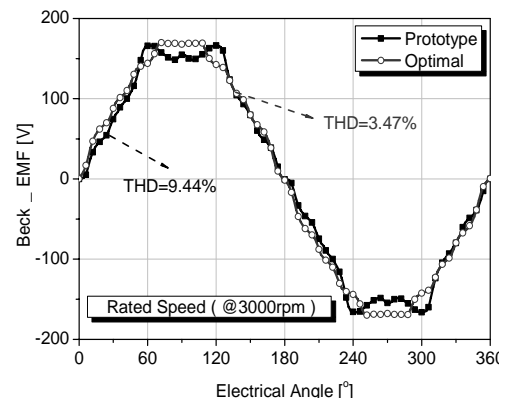


Fig.10 Back e.m.f (THD) results comparison

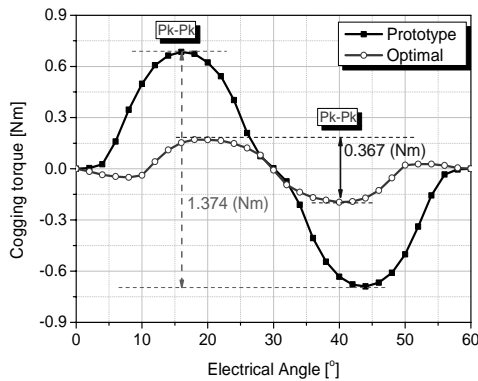


Fig.11 Cogging torque results comparison

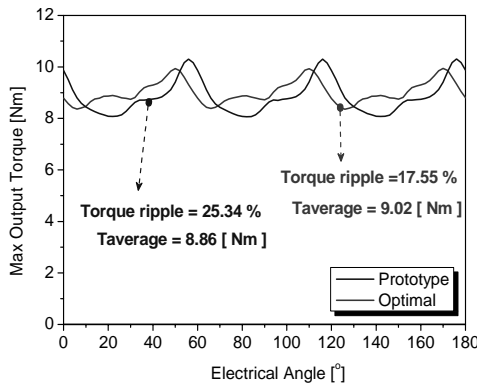


Fig.12 Output torque results comparison

CONCLUSION

In this paper, the torque ripple reduction design of the prototype single layer IPMSM is well achieved through the double layer IPM design in the rotor part. With the help of RSM analysis, the optimal redesigned double layer IPM rotor structure was built, with the obvious improvement of back e.m.f THD and CT characteristics. In the FEM results comparison, the torque ripple of the new designed double layer IPMSM model decreased 30% compared to the prototype model. Therefore, it is well verified that by multi-layer IPM design, the IPMSM performance can be improved effectively. With the present optimization method, other motor performance also can be concerned similarly.

REFERENCES

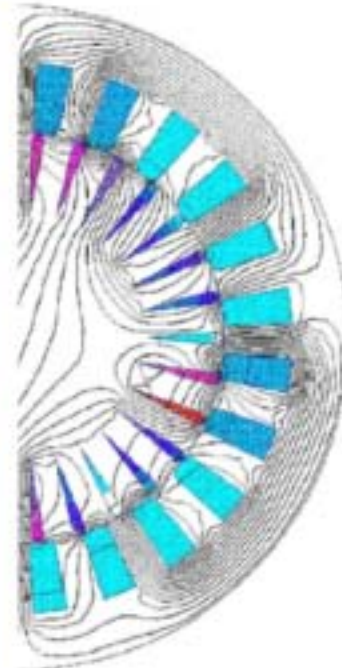
- [1] Nicole Bianchi, Thomas M. Jahns, "Design, Analysis, and Control of Interior PM synchronous Machines", IEEE-IAS Electrical Machines Committee.
- [2] Hong-Seok Ko and Kwang-Joon Kim, "Characterization of Noise and Vibration Source in Interior Permanent-Magnet Brushless DC motors", *IEEE TRANSACTIONS ON MAGNETICS*, Vol. 40, No. 6, November 2004.
- [3] Z.Q.Zhu, S. Ruangsinchaiwanich, N. Schofield and D. Howe, "Reduction of Cogging Torque in Interior-Magnet Brushless Machines", *IEEE TRANSACTIONS ON MAGNETICS*, Vol. 39, No. 5, September 2003
- [4] John M Miller. "Propulsion System for Hybrid Vehicles", *IEE Power and Energy Series 45*.
- [5] Jacek F. Gieras, "Analytical approach to Cogging torque Calculation of PM Brushless Motors", *IEEE Transactions on Industry Application*, Vol. 40, No. 5, September/ October 2004.
- [6] Sung-I Kim, Ji-Young Lee, Young-Kyoun Kim, Jung-Pyo Hong, Yoon Hur, Yeon-Hwan Jung, "Optimization for reduction of torque ripple in

interior Permanent Magnet Motor by using the Taguchi Method", *IEEE Transactions on Magnetics*, Vol 41, No. 5, May 2005.

- [7] Raymond H. Myers, Douglas C. Montgomery, "Response Surface Methodology: Process and Product Optimization Using Designed Experiment", A Wiley-Interscience Publication John Wiley & Sons, INC.

XVII International Conference on Electrical Machines

ICEM 2006



CONFERENCE PAPERS

Browse the ICEM 2006 Full Papers by:

- **Session**
- **Author**

September 2-5, 2006

Chania, Crete Island, Greece

Organising Institutions:



National
Technical
University of
Athens

Technical
University of
Crete

Aristotle
University of
Thessaloniki

University of
Patras

Democritus
University of
Thrace

15:30-16:40 POSTER (DIALOGUE) SESSION PSA1: PERMANENT MAGNET MACHINES

Saturday, September 2nd 2006

No	Ref	Paper title	Authors	Country of the corresponding author
PSA1-1	141	A Permanent Magnet Generator for Small Scale Wind Turbines	J.R. Bumby, N. Stannard and R. Martin	UK
PSA1-2	313	A Method for Dynamic Analysis of an Interior Permanent Magnet Motor Based on Nonlinear Magnetic Circuit	K. Nakamura, M. Ishihara, and O. Ichinokura	Japan
PSA1-3	163	High-speed permanent magnet generators design and testing	Yanush Danilevich, Victor Antipov	Russia
PSA1-4	180	An Attempt to Extend the Flux Weakening Range of a Single Stator Dual Rotor PM Machine	Imen Abdennadher, Ahmed Masmoudi and Ahmed Elantably	Tunisia
PSA1-5	234	Numerical design of DC brush motor with rare-earth magnets for ABS system including tolerances of input parameters	G. Ombach, J. Junak and A. Ackva	Germany
PSA1-6	244	A Stator Turn Fault Tolerant Strategy for Interior PM Synchronous Motor Drives in Safety Critical Applications	Youngkook Lee and T.G. Habetler	USA
PSA1-7	245	Comparative Evaluation of Axial Flux versus Radial Flux Permanent Magnet Synchronous Machines	M. Krishnamurthy, B. Fahimi and K. D. Oglesby	USA
PSA1-8	249	Design and Implementation of a Tubular Brushless DC Motor for Direct-Drive Applications	S.H. Mao, B.J. Lin, and M.C. Tsai	Taiwan
PSA1-9	250	Design of Interior Permanent Magnet Motors for Smoothing Back-EMF Waveform	H.S. Chen and M.C. Tsai	Taiwan
PSA1-10	251	Development of the Discontinuous Primary Permanent Magnet Linear Synchronous Motor	Kenji Suzuki, Yong-Jae Kim, Masaya Watada and Hideo Dohmeki	Japan
PSA1-11	254	Optimised design of concentrated winding PM brushless motors	A. Castagnini, P. Faure Ragani, G. Secondo	Italy
PSA1-12	266	Evaluation of Eddy Current Loss in Tubular Permanent Magnet Motors by Three-Dimensional Finite Element Analysis	J. Chai, J. Wang and D. Howe	UK
PSA1-13	267	Magnetic Field Distribution in Brushless Permanent Magnet AC Motors with Interior Permanent Magnets (IPM) and Slotted Stator	F. Poltschak, W.Amrhein	Austria
PSA1-14	274	A Brushless Permanent Magnet Motor with Hybrid Windings	M. C. Tsai and L. Y. Hsu	Taiwan
PSA1-15	276	Torque ripple reduction design of Multi-layer Interior Permanent Magnet Synchronous Motor by using Response Surface Methodology	Liang Fang, Soon-O Kwon, Peng Zhang, Jung-Pyo Hong	China
PSA1-16	311	Reluctance Network Analysis Model of a Permanent Magnet Generator Considering an Overhang Structure	K. Nakamura, M. Ishihara, and O. Ichinokura	Japan
PSA1-17	312	Multipolar Reluctance Generator Using Stator Core with Permanent Magnet	O. Ichinokura, T. Ono, T. Tashiro, K. Nakamura, and A. Takahashi	Japan
PSA1-18	346	Distribution, coil-span and winding factors for AFPM with concentrated windings	S. E. Skaar, Ø. Krøvel, R. Nilssen	Norway
PSA1-20	284	Application of a Toroidal Harmonic Expansion for Computing the Magnetic Field from a Balanced 6-Pole Permanent-Magnet Motor	J. Selvaggi, S. Salon, O. Kwon, and M.V.K. Chari	USA

11:40-13:20 ORAL SESSION OTM4: TESTING, MEASUREMENTS, ACOUSTIC NOISE AND VIBRATION ASPECTS

Tuesday, September 5th 2006

Ariadne Room

No	Ref	Paper title	Authors	Country of the corresponding author
OTM4-1	320	Testing of Electric Machines with a Dedicated System for Data Acquisition and Processing	Voicu Groza, Marius Biriescu, Vladimir Crețu, Gheorghe Liuba, Martián Mot , Gheorghe Madescu	Romania
OTM4-2	197	The increase of the magnetic noise of induction motors due to the low order excitation modes generated by the rotor eccentricity	S.L. Nau, R. Beck, H.L.V. dos Santos, N. Sadowski, R. Carlson	Brazil
OTM4-3	452	Monitoring of Induction Motors Rotor Faults by non invasive sensors	A. Bellini, C. Conconi, G. Franceschini, C. Tassoni, A. Toscani	Italy
OTM4-4	505	Acoustic Noise and Displacement Analysis of a 3-phase Transformer Core Under Sinusoidal and PWM Excitations	X G Yao, Thant P P Phway, A J Moses, F Anayi	UK
OTM4-5	546	Optimal Design to reduce Acoustic Noise in Interior Permanent Magnet Motor using Response Surface Methodology	Sang-Ho Lee, Suk-Hee Lee, Jung-Pyo Hong, Sang-Moon Hwang, Ji-Young Lee, and Young-Kyoun Kim	Korea

15:30-16:40 POSTER (DIALOGUE) SESSION PSA1: PERMANENT MAGNET MACHINES

Saturday, September 2nd 2006

No	Ref	Paper title	Authors	Country of the corresponding author
PSA1-1	141	A Permanent Magnet Generator for Small Scale Wind Turbines	J.R. Bumby, N. Stannard and R. Martin	UK
PSA1-2	313	A Method for Dynamic Analysis of an Interior Permanent Magnet Motor Based on Nonlinear Magnetic Circuit	K. Nakamura, M. Ishihara, and O. Ichinokura	Japan
PSA1-3	163	High-speed permanent magnet generators design and testing	Yanush Danilevich, Victor Antipov	Russia
PSA1-4	180	An Attempt to Extend the Flux Weakening Range of a Single Stator Dual Rotor PM Machine	Imen Abdennadher, Ahmed Masmoudi and Ahmed Elantably	Tunisia
PSA1-5	234	Numerical design of DC brush motor with rare-earth magnets for ABS system including tolerances of input parameters	G. Ombach, J. Junak and A. Ackva	Germany
PSA1-6	244	A Stator Turn Fault Tolerant Strategy for Interior PM Synchronous Motor Drives in Safety Critical Applications	Youngkook Lee and T.G. Habetler	USA
PSA1-7	245	Comparative Evaluation of Axial Flux versus Radial Flux Permanent Magnet Synchronous Machines	M. Krishnamurthy, B. Fahimi and K. D. Oglesby	USA
PSA1-8	249	Design and Implementation of a Tubular Brushless DC Motor for Direct-Drive Applications	S.H. Mao, B.J. Lin, and M.C. Tsai	Taiwan
PSA1-9	250	Design of Interior Permanent Magnet Motors for Smoothing Back-EMF Waveform	H.S. Chen and M.C. Tsai	Taiwan
PSA1-10	251	Development of the Discontinuous Primary Permanent Magnet Linear Synchronous Motor	Kenji Suzuki, Yong-Jae Kim, Masaya Watada and Hideo Dohmeki	Japan
PSA1-11	254	Optimised design of concentrated winding PM brushless motors	A. Castagnini, P. Faure Ragani, G. Secondo	Italy
PSA1-12	266	Evaluation of Eddy Current Loss in Tubular Permanent Magnet Motors by Three-Dimensional Finite Element Analysis	J. Chai, J. Wang and D. Howe	UK
PSA1-13	267	Magnetic Field Distribution in Brushless Permanent Magnet AC Motors with Interior Permanent Magnets (IPM) and Slotted Stator	F. Poltschak, W.Amrhein	Austria
PSA1-14	274	A Brushless Permanent Magnet Motor with Hybrid Windings	M. C. Tsai and L. Y. Hsu	Taiwan
PSA1-15	276	Torque ripple reduction design of Multi-layer Interior Permanent Magnet Synchronous Motor by using Response Surface Methodology	Liang Fang, Soon-O Kwon, Peng Zhang, Jung-Pyo Hong	China
PSA1-16	311	Reluctance Network Analysis Model of a Permanent Magnet Generator Considering an Overhang Structure	K. Nakamura, M. Ishihara, and O. Ichinokura	Japan
PSA1-17	312	Multipolar Reluctance Generator Using Stator Core with Permanent Magnet	O. Ichinokura, T. Ono, T. Tashiro, K. Nakamura, and A. Takahashi	Japan
PSA1-18	346	Distribution, coil-span and winding factors for AFPM with concentrated windings	S. E. Skaar, Ø. Krøvel, R. Nilssen	Norway
PSA1-20	284	Application of a Toroidal Harmonic Expansion for Computing the Magnetic Field from a Balanced 6-Pole Permanent-Magnet Motor	J. Selvaggi, S. Salon, O. Kwon, and M.V.K. Chari	USA

10:20-11:30 POSTER (DIALOGUE) SESSION PTM2: DRIVES OF SYNCHRONOUS, PM AND DC MACHINES

Tuesday, September 5th 2006

No	Ref	Paper title	Authors	Country of the corresponding author
PTM2-1	526	Operational Behaviour of Industrial DC Drives in Paper Machines in Relation to Elastic Shafts Characteristics	C. Michael, A. Safacas	Greece
PTM2-3	344	Accurate Torque Control of VSI Fed Synchronous Machine Under Normal or Fault Conditions Using Discrete Modelling of Airgap Flux	M. Bekemans, F. Labrique, E. Matagne	Belgium
PTM2-4	702	Brushless, Self-Excited Synchronous Field-Winding Machine for Variable-Speed Drive Applications	Alexander Rovnan, Heath Hofmann	USA
PTM2-5	128	The New Methodology Of The Power Loss Calculation Under Deformed Flux Conditions	Z. Gmyrek, A. Boglietti, A. Cavagnino	Poland
PTM2-6	415	AC High Dynamometer for testing motor drive system	Gildong Kim, Hanmin Lee, Sehchan Oh, Sunghyuk Park, Changmu Lee	Korea
PTM2-7	341	Fast Prototyping of Vector Controllers for Interior PM Synchronous Motors	M. Tursini, A. Scotti, D. D'Antonio, and E. Chiricozzi	Italy
PTM2-8	379	Current Waveform Analysis of PWM Inverter-Fed Permanent Magnet Synchronous Machine Accounting for Cross-Magnetization	M. Kimura, K. Ide, H. Mikami	Japan
PTM2-9	342	Sensorless Control of PM Synchronous Motors with Luenberger Observer: Theoretical Issues and Implementation Results	M. Tursini, A. Scafati, R. Petrella	Italy
PTM2-10	460	Speed Control of Permanent Magnet Synchronous Motors by Current Vector Control	P. Fernandez, J. A. Goemes and A. M. Iraolagoitia	Spain
PTM2-11	626	Line-Start Permanent-Magnet Chemical Pump Drives	A.C. Smith and E.Peralta Sanchez	UK
PTM2-12	237	Versatile High Torque Direct Drive with PM-Excitation and Duplex Stator Arrangement	W.-R. Canders, H. Mosebach, M. R. Rezaei	Germany
PTM2-13	257	A Novel Drive Strategy for Vibration Suppression in Permanent Magnet Brushless DC Motor	Tao. Sun, Gen-Ho Lee, Jeng-Pyo Hong	Korea
PTM2-14	129	Implementation of an active converter for high quality dc drive performance	N.N. Barsoum, S.K. Wong	Malaysia
PTM2-15	155	Controlled DC Electric Drive Based on Stochastic Calculation Techniques	Achmad Alyan and Raul Rabinovici	Israel
PTM2-16	307	Determination of the Optimum Power Factor and Efficiency of a Characteristic DC Drive System via Simulation	K. Georgakakos, A. Safacas, I. Georgakopoulos	Greece
PTM2-17	440	Optimal Integral State Feedback controller for a DC motor	H. Delavari, GH. Alizadh, M. Sharifan,	Iran
PTM2-18	255	Simplified sensorless control technique for wound rotor synchronous motor	F. Chabour, J. P. Vilain, P. Macret, P. Masson, L. Kobylansky	France